Aging and degradation of lithium-ion batteries

9

N. Omar[1], Y. Firouz[1], H. Gualous[2], J. Salminen[3], T. Kallio[4], J.M. Timmermans[1], Th. Coosemans[1], P. Van den Bossche[1], J. Van Mierlo[1]
[1]Vrije Universiteit Brussel, Brussels, Belgium; [2]Université de Caen Basse Normandie, Cherbourg-Octeville, France; [3]VTT Technical Research Centre of Finland, Espoo, Finland; [4]Aalto University, Espoo, Finland

9.1 Introduction

Since the beginning of the automobile era, the internal combustion engine (ICE) has been used for vehicular propulsion. In addition, motor vehicles powered by the ICE are significant contributors to air pollutants and greenhouse gasses linked to global climate change [1,2]. As the global economy begins to strain under the pressure of rising petroleum prices and environmental concerns, research has spurred the development of various types of clean energy transportation systems such as hybrid electric vehicles, battery electric vehicles, and plug-in hybrid electric vehicles [3,4]. When establishing energy storage technologies one has to consider critical aspects such as the output power during acceleration, the efficient use of the regenerative energy and the life cycle; no current battery technology can meet these often-concurrent objectives [4–7]. In the last decade, lithium-ion battery technology has acquired considerably high attention due to the beneficial performances in terms of energy, power, and life cycle compared to lead-acid and nickel metal-hydride batteries [8,9].

The term *lithium-ion* encompasses a number of chemistries based of the materials used in the anode and cathode.

It is generally well known that the lifetime of a battery is the key issue in the assessment of the most appropriate battery technology in environmental friendly vehicles [10,11]. In Ref. [12], an extended life cycle analysis has been performed for graphite anode/lithium iron phosphate cathode (C/LFP) batteries. The analysis concluded that C/LFP has a generally long life cycle. In addition to this work, Omar [13] performed a number of life cycle tests on different lithium-ion battery brands and chemistries. They observed that the cycle life of LFP and lithium titanate oxide anode/graphite cathode batteries (LTO/C) are longer than lithium nickel manganese cobalt oxide (C/NMC) or lithium nickel cobalt aluminum oxide (C/NCA) batteries.

Following these studies, Wang *et al.* [14] developed a similar life cycle model for C/LFP batteries. The model has been developed based on statistical experimental results, whereby the proposed battery has been cycled at different operating conditions for ambient temperature, current rates, and depth of discharge. The model gives good results in the investigated operating range.

Rechargeable Lithium Batteries. http://dx.doi.org/10.1016/B978-1-78242-090-3.00009-2

However, from these studies, we can conclude that these works were limited to cycle life and the impact of calendar life was not considered.

Eddahech *et al*. [15] performed a calendar life evaluation for a C/NMC (12 Ah) battery at different operating conditions (30, 45, and 60 °C; 30% state of charge (SoC), 65% SoC, and 100% SoC). They concluded that the lifetime of the battery decreases the more the working temperature and SoC increases. In addition, they observed that the main contributors to aging are the increase of the internal resistance and capacity degradation. In Ref. [16], it is documented that the degradation is due to the loss of the active and mainly cyclible lithium ions. Furthermore, the growths of the solid electrolyte interface (SEI) and decline of the electrolyte conductivity are the major fading mechanisms [17]. These results have been also confirmed by Zhang and White [18] through experimental data and numerically with a single particle model. From their analysis, they concluded that the battery fading mechanisms changes nonlinearly as a function of the working temperature.

However, Kassem *et al*. [19] carried out a similar analysis on C/LFP batteries and they concluded that the capacity fade at higher working temperatures is attributed to the side reactions that take place at anode level due to the decomposition of the solvent, which leads to the growth of the SEI. However, the side reactions at the cathode level are less prominent than at the anode level.

From all these studies, we can conclude that the behavior of lithium-ion batteries, in particular for C/LFP batteries during calendar life at different storage conditions, is not well identified because the investigation works are only performed at high operating temperatures and, thus, an extended analysis in a wide operating window is still unknown. Therefore, there is a need for having a comprehensive analysis whereby the experimental data should be combined with numerical tools and postmortem analysis for having a clear overview of battery behavior.

9.2 Methodology

In order to have a clear view of battery behavior during calendar life, in the framework of this study, the methodology as presented by Figure 9.1 has been proposed.

As we can observe, the investigated batteries (C/LFP 7 Ah, pouch) have been investigated at working temperatures (60, 40, 25, 10, 0, and −10 °C) and different SoC levels (100%, 75%, 50%, and 25%).

The batteries have been stored at these conditions during 44 weeks (with inspection at 75% SoC, which was at 32 weeks). Every 4 weeks, the battery performances were checked by standard procedures at 25 °C based on both a capacity test and a hybrid pulse power characterization (HPPC) test for evaluation of the change in the internal resistance.

The capacity test was done at 1 I_t[1] charging (constant current constant voltage[2]) and then followed by the discharge step at 1 I_t until the minimum voltage (2 V) was reached. The rest time between the charge and discharge steps was 30 min.

[1] The current I_t represents the discharge current in amperes during 1 h discharge and C is the measured capacity of a cell as specified in the standard IEC 61434 [20,21].

[2] Constant current constant voltage: the batteries have been charged at 1 I_t until 3.65 V and then the voltage has been kept constant at 3.65 V until the current has been decreased to 0.7 A.

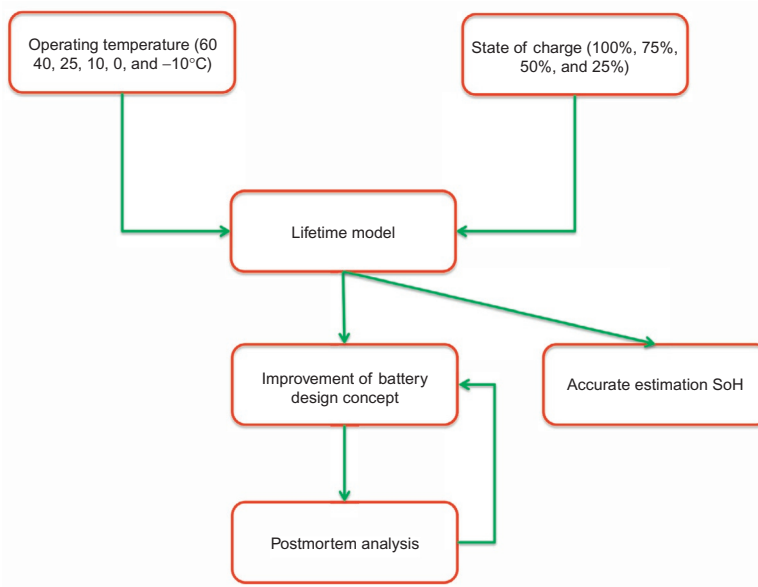

Figure 9.1 Used methodology.

Regarding the HPPC protocol, the test was carried out at different current rates (0.33 I_t, 1 I_t, 2 I_t, 3 I_t, 5 I_t, 7 I_t) from 100% SoC to 0% SoC with steps of 5% SoC. The charge and discharge HPPC pulses were 10 s.

In this study, the evolution of the capacity degradation and the internal resistance were investigated and analyzed.

Once the batteries reach their end of life (80% of the measured rated capacity), batteries will undergo postmortem analysis for better understanding of the physical aging phenomena inside the batteries.

9.3 Results

9.3.1 Capacity degradation

Figures 9.2–9.5 show the results of the capacity evolution as a function of the storage time at different SoC levels and storage temperatures.

As we generally can observe, the battery capacity decreases faster the higher the SoC of the battery. As an example, the capacity degradation at 40 °C storage temperature is 20% after 25 weeks, 20% after 28 weeks, and 19% after 44 weeks at 100% SoC, 50% SoC, and 25% SoC, respectively. This evolution also can be found at the other storage temperatures (60, 25, 10, 0, and −10 °C). However, the impact of the storage temperature is more significant than the SoC level. When we compare

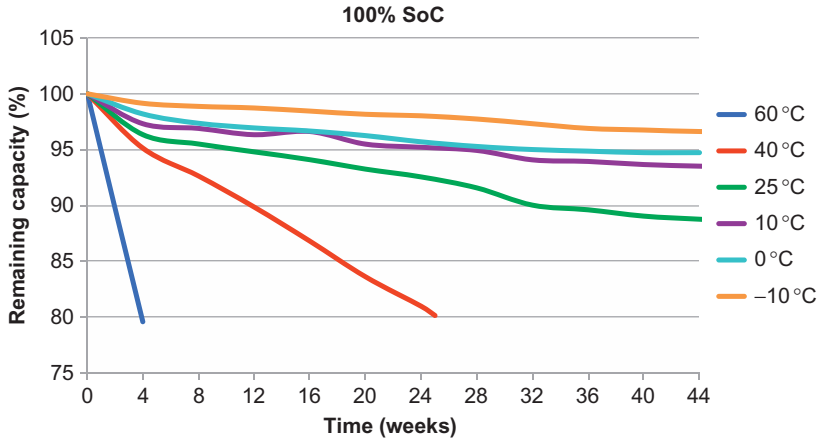

Figure 9.2 Evolution of capacity degradation versus storage time at 100% SoC.

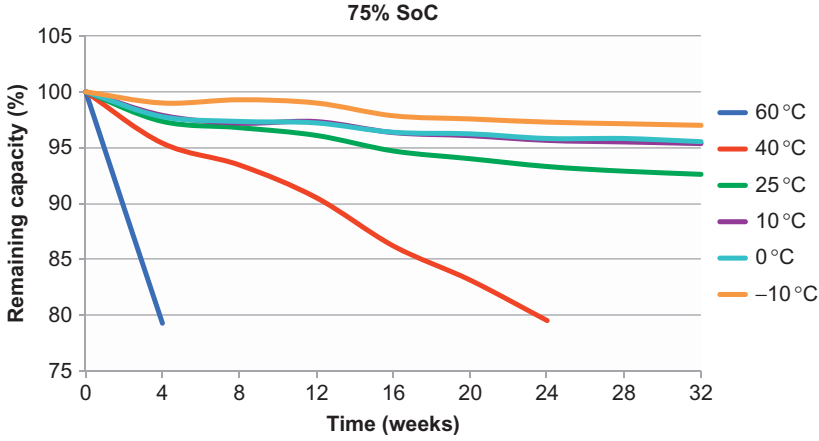

Figure 9.3 Evolution of capacity degradation versus storage time at 75% SoC.

the mutual results, one can recognize for example at 50% SoC, the capacity degradation is 20% after 5 weeks, 20% after 28 weeks, 8% after 44 weeks, 1% after 44 weeks, and 0% after 44 weeks at storage temperatures 60, 40, 25, 10, 0, and −10 °C, respectively. Therefore, in general we can conclude that the impact of the storage temperature is more harmful than the SoC level, as shown in Figure 9.4.

From this point of view, it is clear that from the control strategy of the battery system and the vehicle that the battery needs to be kept at the desired storage temperature and SoC level when it will not be used for a long period.

The above-indicated results also have been confirmed by many researchers [22–24]. In Refs. [22–26], it is reported that the capacity degradation at higher temperatures is mainly attributed to the formation of the SEI growth as a function of time.

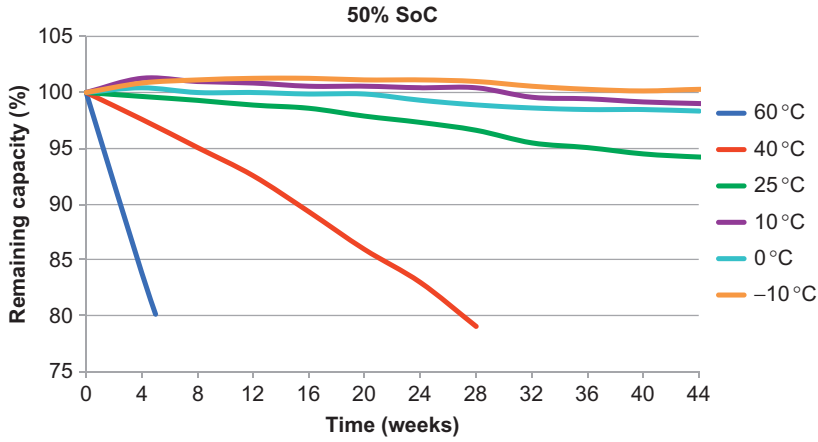

Figure 9.4 Evolution of capacity degradation versus storage time at 50% SoC.

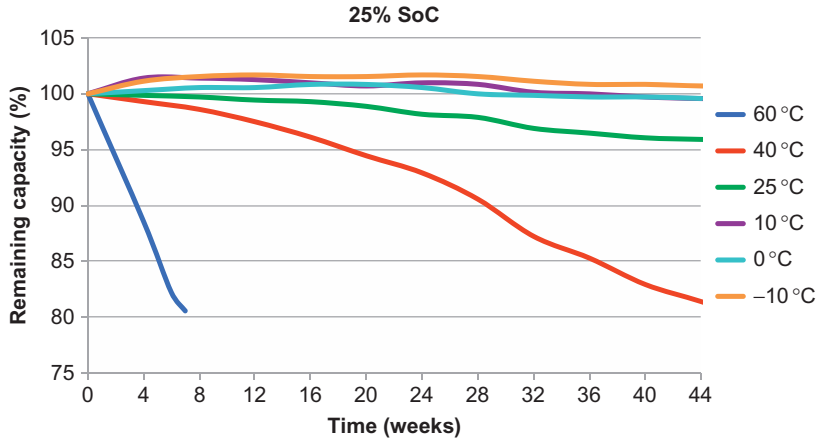

Figure 9.5 Evolution of capacity degradation versus storage time at 25% SoC.

It was also concluded that the resistance of the battery increases and that the growth of SEI leads to a square root time dependency. Researchers at Aachen University [25] concluded that capacity fades at higher SoC levels, which implies huge overpotential at the electrode/electrolyte interface, and that calendar life can be modeled using $t^{0.75}$ dependency [25].

The presented results in Figures 9.2 through 9.5 indicate that capacity degradation for the investigated battery type in this study shows an exponential relationship as a function of the storage time expressed by Equation (9.1):

$$\text{Capacity degradation}\,(t) = ae^{(bt_{\text{stor}})} + c^{(dt_{\text{stor}})} \tag{9.1}$$

9.3.2 Evolution of battery behavior based on impedance spectroscopy

In Section 9.3.1, the evolution of battery behavior based on capacity tests has been investigated. The experimental results show that the storage temperature has a significant impact on battery capacity degradation. However, the results could not reveal if the obtained results are due to specific physical changes in the battery. Therefore, in this section, the battery characteristics have been investigated based on electrochemical impedance spectroscopy (EIS) to examine this issue. For this purpose, the measurements have been conducted on an EIS potentiostat of Bio-Logic HCP-1500. The battery cells have been characterized every 4 weeks at 25 °C at the proposed SoC conditions as mentioned earlier in Section 9.2. The measurements have been carried out from 10 kHz to 50 mHz.

Generally, the EIS response can be considered as inductive at high frequencies and capacitance at low frequency. The first one represents more the metal connectors while the second one stands for the charge transfer phenomena.

Figures 9.6–9.10 show the Nyquist plot, whereby the imaginary part of the impedance is expressed as a function of the real part. From these results, one can indicate that the ohmic resistance of the cell (interfacial impedance) increases at higher storage temperatures during the calendar life of the battery. The ohmic resistance based on the Nyquist plot represents the intersection of the impedance with the x-axis. However, the variation on this parameter decreases the more the storage temperature goes down. The observation obtained is completely in line with the results in Section 9.3.1. Furthermore, the Nyquist plots show that the imaginary part of the impedance is

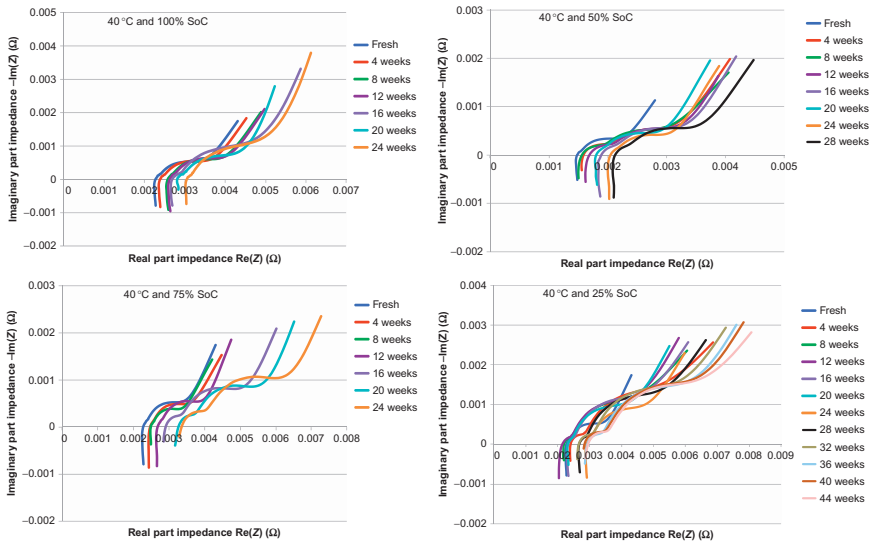

Figure 9.6 Evolution of battery behavior at 40 °C calendar life based on impedance spectroscopy.

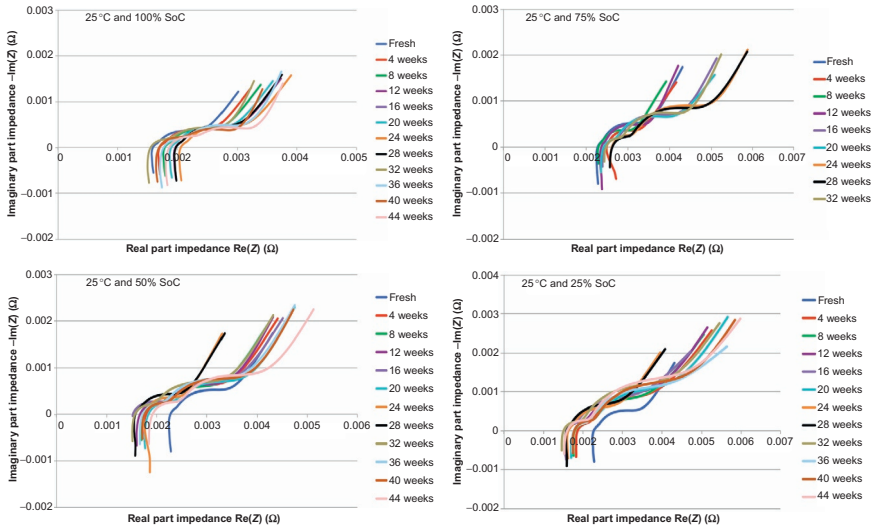

Figure 9.7 Evolution of battery behavior at 25 °C calendar life based on impedance spectroscopy.

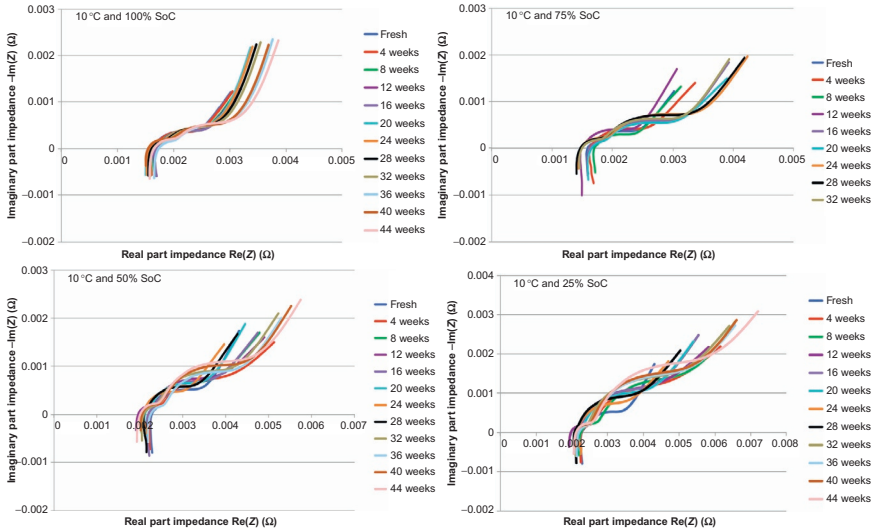

Figure 9.8 Evolution of battery behavior at 10 °C calendar life based on impedance spectroscopy.

changing during calendar life. This indicates that the capacitance of the battery decreases based on the following relationship:

$$\mathrm{Im}(Z) = \frac{1}{2\pi f C(f)} \tag{9.2}$$

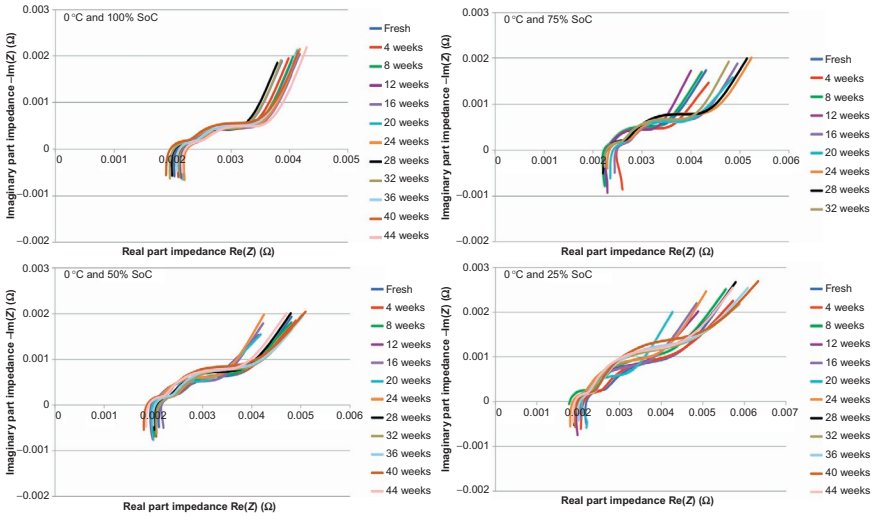

Figure 9.9 Evolution of battery behavior at 0 °C calendar life based on impedance spectroscopy.

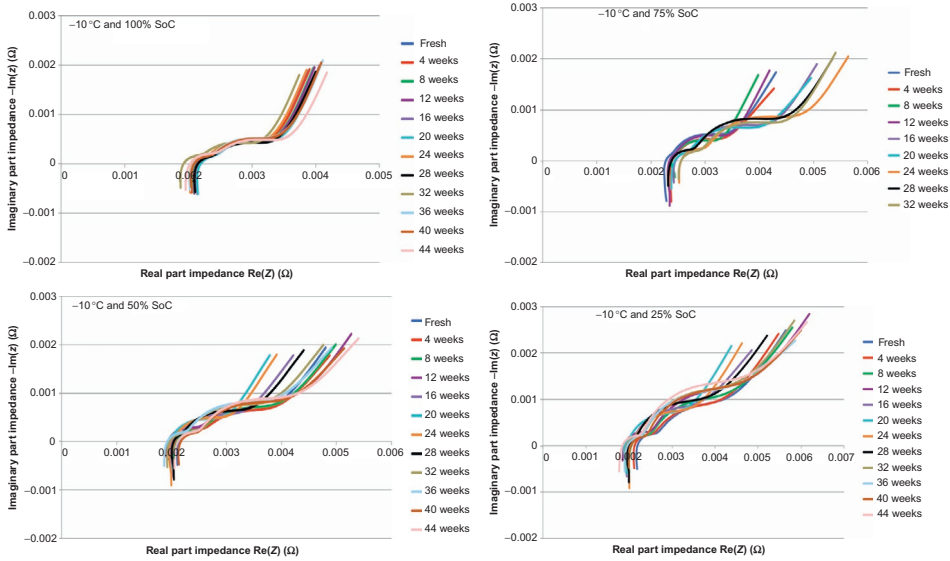

Figure 9.10 Evolution of battery behavior at −10 °C calendar life based on impedance spectroscopy.

where f represents the frequency, C is the capacitance, and Im(Z) the imaginary part of the impedance.

In Refs. [27,28], it is documented that the capacitance characteristic is related to the surface phenomena that occur mostly on the negative electrode. If the charge transfer

resistance increases, which represents the semicircle in the Nyquist plot, this implies that the access time of the lithium-ion to the surface is longer. This observation confirms that the SEI layer growths, which contribute to internal resistance, increase and capacity degradation as a consequence. This result has been confirmed by [18] for graphite/lithium cobalt oxide pouch cells. They observed that storing the battery at high temperatures implies that some electroactive surface area becomes inaccessible due to side reactions and isolation of particles from the electrode surface. In addition, these results have been confirmed as well at half-cell level by Ref. [29].

Furthermore, from this analysis it is notable that the variation in the plots becomes smaller the more the storage temperature decreases. This results in the conclusion that the formation of the SEI layer at lower temperature grows less fast. From this point of view, the SEI consumes more lithium-ion and electrolyte decomposition accelerates at higher temperatures, which results to lower conductivity as well. These results have been confirmed by Ref. [30].

Here, it should be noted that according to the Nyquist plot the ohmic resistance (interfacial impedance) changes during the calendar life, storage temperature, and SoC. At lower SoC levels, the semicircle becomes wider and, thus, the charge transfer resistance increases. This means that the battery characteristics from the modeling point of view changes. This leads to the conclusion that development of an appropriate battery model, which is able to predict the battery behavior at different operating conditions, is complicated.

9.3.3 Changes of battery models parameters

In this section, the earlier-performed analysis has been extended, whereby the battery behavior has been analyzed based on the evolution of the model parameters. Therefore, the FreedomCar battery model has been used as shown in Figure 9.11. The FreedomCar battery model consists of the open circuit voltage, ohmic resistance R_o, polarization resistance R_p, and polarization capacitance C.

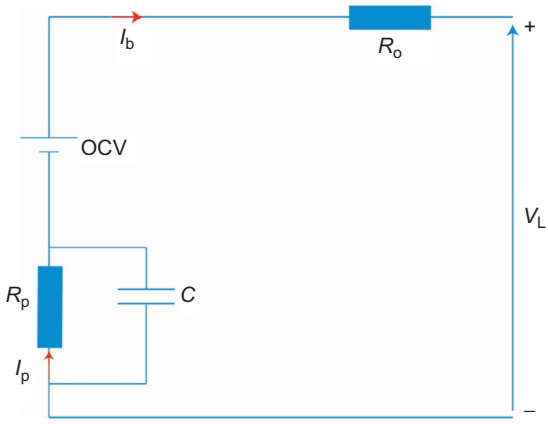

Figure 9.11 First order FreedomCar battery model [12].

Prior to starting with estimation of battery model parameters, the batteries have been characterized based on the HPPC using 10 s pulses as illustrated in Figure 9.12 [13]. In order to evaluate the model parameters as to function of current rate and SoC, the test has been repeated at the current rates and SoC values as specified in Section 9.2. However, in this study the results of the model parameters at 50% SoC and current level 5 I_t are proposed.

The first results of the HPPC test are shown in Figures 9.13–9.16. In these figures, the total resistance during the 10 s pulse is summarized. From the obtained results one

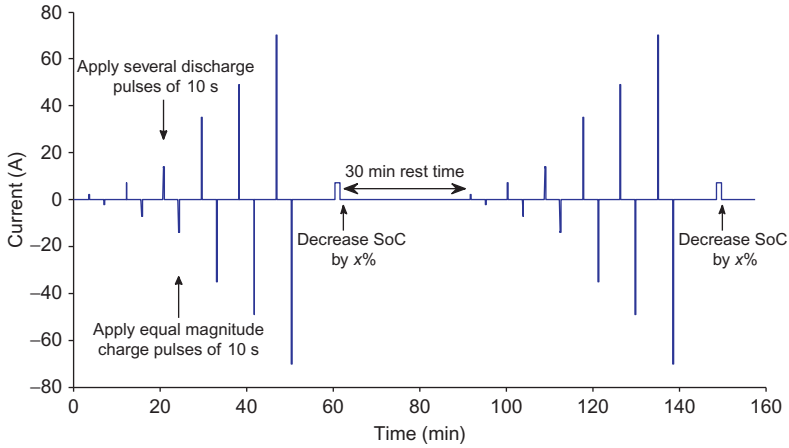

Figure 9.12 Hybrid pulse power characterization test.

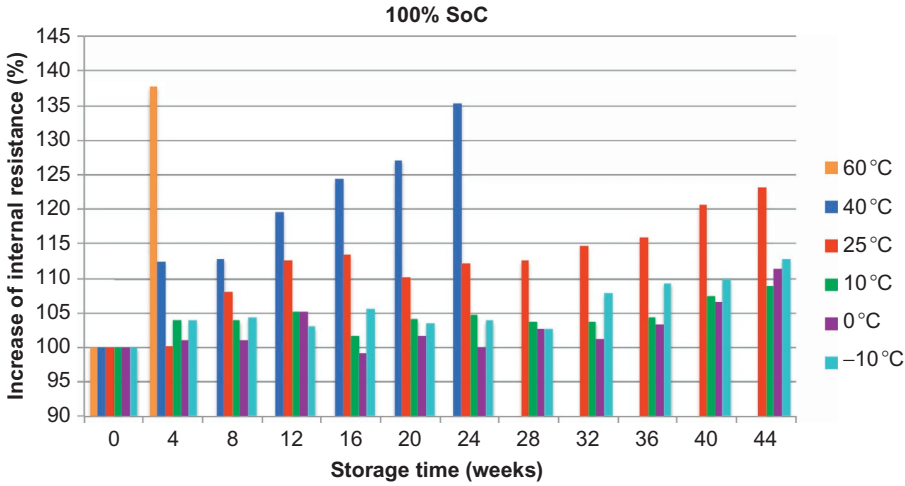

Figure 9.13 Evolution of internal resistance versus time at 100% SoC.

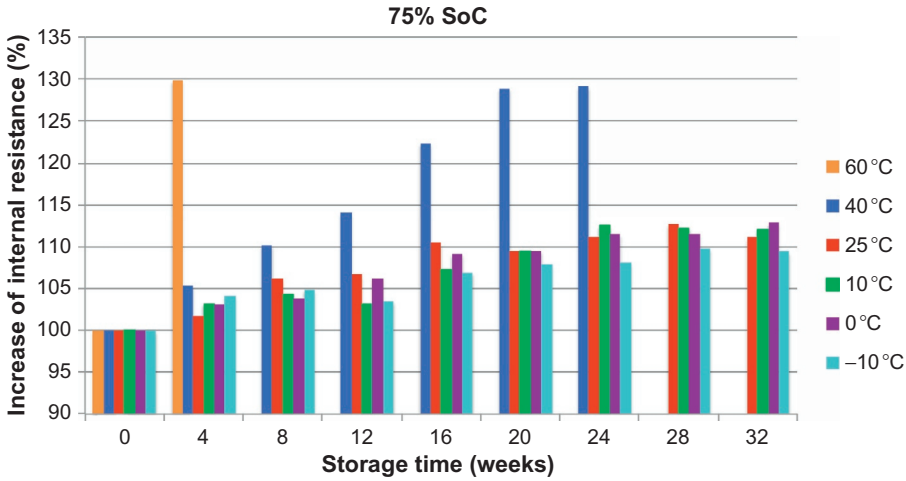

Figure 9.14 Evolution of internal resistance versus time at 75% SoC.

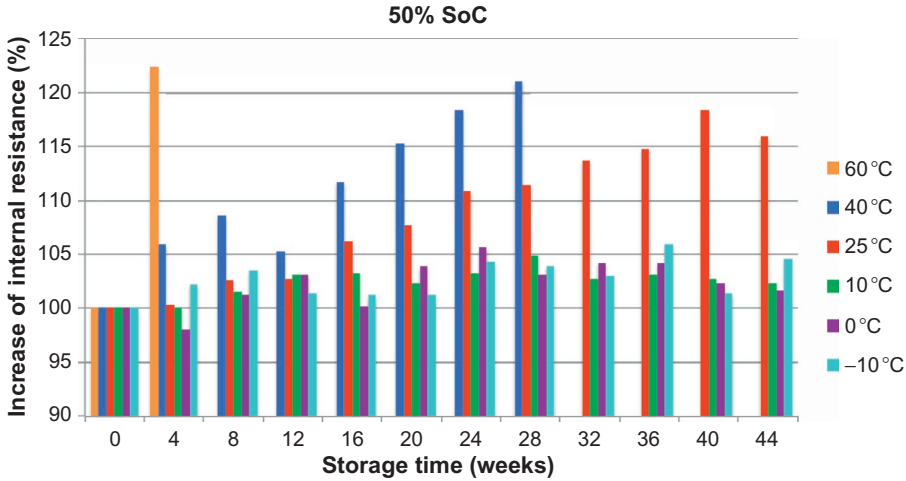

Figure 9.15 Evolution of internal resistance versus time at 50% SoC.

can notice that the internal resistance of the battery is changing remarkably. The increase of the resistance is particularly notable at higher storage temperatures and SoC levels. The increase of the resistance at 100% SoC and 40 °C is 135% after 24 weeks compared to 123% at 25 °C after 44 weeks. Here it should be noted that the battery at 25 °C does not reach its end of life. Furthermore, the increase of the resistance becomes smaller the more the storage temperature decreases. These results are in line with the performed capacity test and EIS measurements. In addition, these results have been confirmed by many studies [19–33].

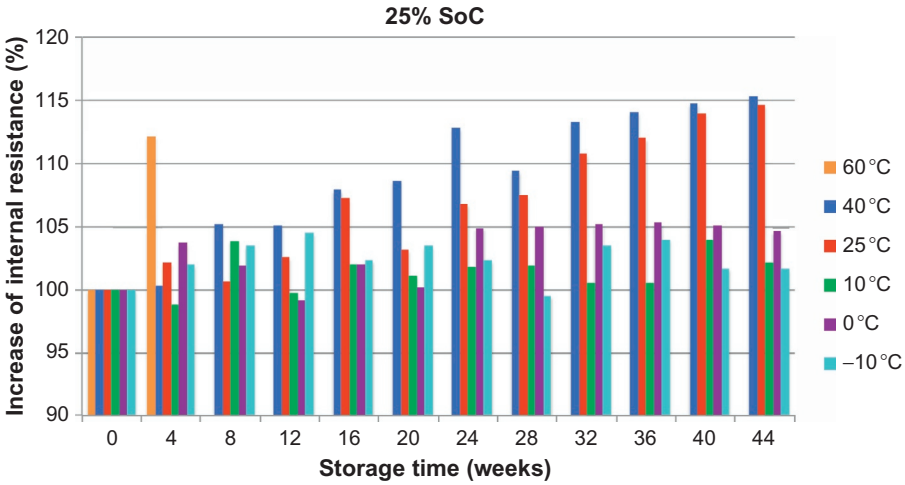

Figure 9.16 Evolution of internal resistance versus time at 25% SoC.

Kassem *et al*. [19] concluded that the decrease of the capacity is more prominent at higher storage temperatures. They conducted similar analyses at SoC levels (30%, 65%, and 100%) and storage temperatures (30, 45, and 60 °C). All examined batteries showed significant capacity fade at temperatures exceeding 30 °C. Lithium-ion loss has been identified as the source of capacity fade. This fade has been attributed to the side reactions that occur at the anode level, where electrolyte decomposition occurs and the SEI layer grows. A bigger SEI layer results in higher internal resistance, as we also observed based on our results.

However, Zhang and White [18] concluded that the lithium-ion loss is not the only source for capacity fading and increase of internal resistance. They observed that there is also a dramatic decrease of the active material. Such decrease has been related to loss of contacts between the particles during the storage test. This observation also has been confirmed by Ref. [29] at the half-cell level. These measurements were based on lithium cobalt oxide ($C/LiCoO_2$)-based batteries, which are more sensitive to higher operating temperatures versus $C/LiFePO_4$.

Dupré *et al*. [31] performed an extended analysis on $C/LiFePO_4$ batteries based on the MAS–NMR technique (magic angle spinning–nuclear magnetic resonance spectroscopy) to investigate the formation of species on the surface of the electrode. They came to the conclusion that the increase of the storage temperature (e.g., 55 °C in their case and for the investigated $C/LiFePO_4$ battery at ± 3.2 V) accelerates the formation of organic species in the surface of the electrode. However, after 1 month of investigation no passivation state was observed. The organic species results from bad particle contacts and inhomogeneous aging on the surface of the electrode. In addition, this process is also associated with unequal potential distribution and an unstable electrochemical process as a consequence.

Following this study, Wohlfahrt-Mehrens *et al*. [32] concluded that capacity fade and increase of internal resistance at higher temperatures is mostly attributed to structural changes and side reactions with the electrolyte, which leads to the formation of salt and H_2O impurities in the electrolyte. However, the results cannot be generalized, as the research has been done based on the lithium manganese oxide battery ($C/LiMn_2O_4$). Also, the composition of the electrolyte itself has a huge effect on the degradation mechanisms. Different organic electrolyte mixtures are used for different electrode materials specifically to optimize performance and longevity.

Käbitz *et al*. [33] performed a similar study on $C/LiNi_{1/3}Mn_{1/3}Co_{1/3}O_2$ batteries and they found that storing the batteries at 50% SoC and at storage temperature 60 °C results to exponential capacity fade and internal resistance increase. They observed as well that the increase of the resistance at 60 °C is 150% higher than at 25 °C after 400 days of calendar life. By comparing their results with ours, one can observe that the increase of the internal resistance is smaller. This difference is related to the different type of batteries that have been investigated. In addition, in our case, operating conditions of the battery cathode lie in the stable working window of the electrolyte. However, for the proposed batteries in the study of Käbitz *et al*. the charge voltage is 4.2 V, which is close to the upper limit of stability potential of the electrolyte. Then, at higher storage temperatures, dissolution of Mn into electrolyte occurs resulting in higher capacity fade and internal resistance increase.

Another remarkable observation is the fact that the increase of the internal resistance is a function of the SoC level. In Figures 9.13 through 9.16 the resistance increase at 25 °C, for example, after 44 weeks, is 23% at 100% SoC, 15% at 50% SoC, and 14% at 25% SoC. Here, it can be observed that the impact of SoC is less determinative than the storage temperature. However, when high SoC and high storage temperatures are combined as can be seen in Figure 9.13, the increase of the internal resistance can be high and the evolution of the resistance can be highly nonlinear. From this point of view, the development of an accurate calendar life model in a wide operating range becomes difficult. These results also have been confirmed and observed by Refs. [16,32,33].

From this point of view, in order to guarantee long lifetime of the battery, the battery should be kept in the most optimal conditions, where capacity fade and increase of internal resistance are small. This leads further to the conclusion that the prediction of the state of health of the battery based on the obtained results is not evident. An appropriate method to estimate this issue is to include both studied parameters (capacity fade and internal resistance) into account as proposed in Ref. [12].

In order to have a complete view of the changing parameters inside the battery during the calendar life, the model parameters as proposed in Figure 9.11 at 25 °C and at 100% and 50% SoC levels have been investigated and compared.

In Figures 9.17 and 9.18, the evolution of the ohmic and polarization resistances and time constant are demonstrated during the calendar life. In the proposed figures it is remarkable that the change of the time constant is almost negligible. However, the increase of the ohmic and polarization resistances is higher. The increase is 109% and 135% for polarization and ohmic resistances, respectively, at 100% SoC. At 50% SoC, the increase is 114% and 119% for polarization and ohmic resistances, respectively.

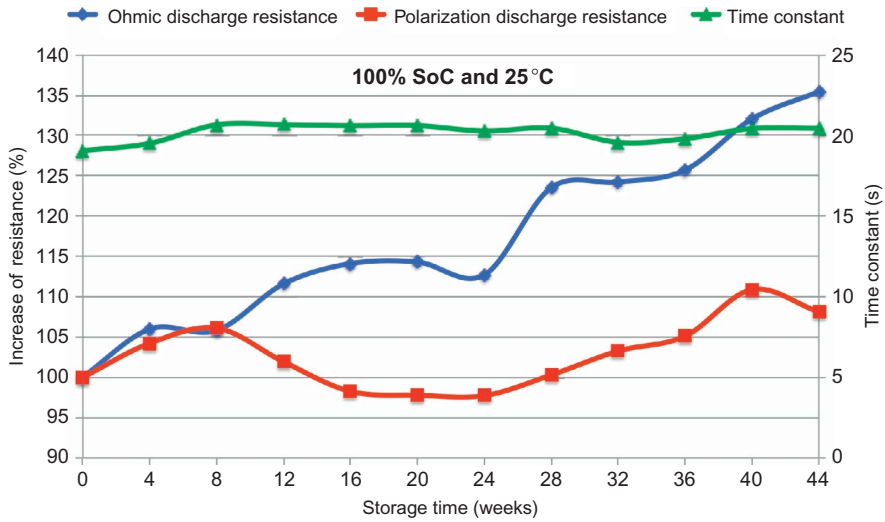

Figure 9.17 Battery model parameters change at storage temperature 25 °C and 100% SoC.

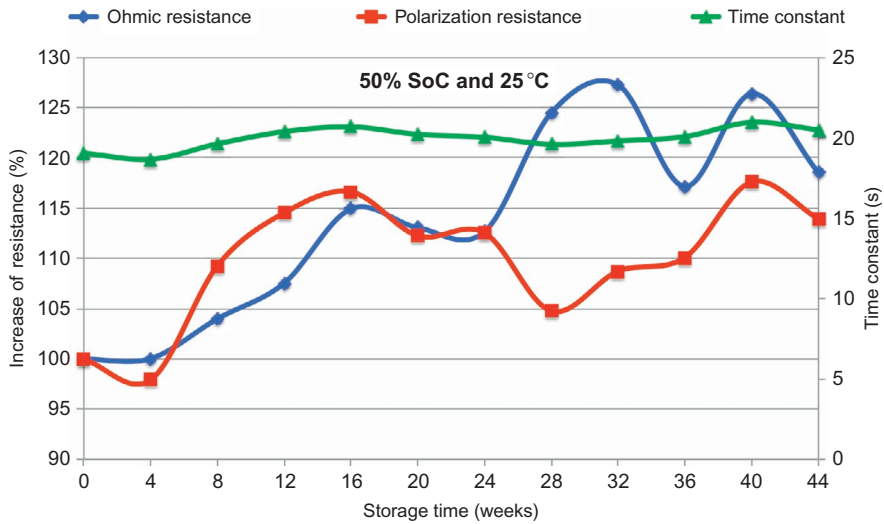

Figure 9.18 Battery model parameters change at storage temperature 25 °C and 50% SoC.

From these results, we can conclude that the increase of ohmic resistance is higher than the polarization resistance. This leads to the conclusion that the increase of the resistance confirms the degradation of the active material inside the battery. Then, from the electrical modeling point of view, the time constant can be assumed as constant. However, the polarization and ohmic resistances evolutions should be included

in the model. Regarding the state of health prediction, the ohmic resistance and the capacity degradation can be assumed as the most critical parameters. In order to have a clear understanding of the evolution of these performance parameters, there is a need for a postmortem.

9.4 Conclusions

In this study, the calendar life characteristics of a 7 Ah lithium iron phosphate pouch cell have been investigated at various temperatures (60, 40, 25, 10, 0, and −10 °C) and SoC levels (100%, 75%, 50%, and 25%).

The experimental results indicate the capacity degradation is more determinative at higher temperatures. Higher states of charge levels accelerate the capacity fade.

Furthermore, the experimental results showed that higher temperatures accelerate the increase of the total internal resistance. These results can be attributed to the occurrence of parasitic reactions, whereby the loss of active material and lithium-ion are the main sources. In addition, the decomposition of the electrolyte and the evolution of the SEI layer are also major contributors to the increase of the internal resistance.

References

[1] J. Van Mierlo, G. Maggetto, E. Van De Burgwal, R. Gense, Driving style and traffic measures influences vehicle emissions and fuel consumption, Proc. Inst. Mech. Eng. D: J. Automob. Eng. 218 (1) (2003) 43–50.

[2] J. Van Mierlo, G. Maggetto, et al., Comparison of the environmental damage caused by vehicles with different alternative fuels and drive trains in a Brussels context, Proc. Inst. Mech. Eng. D: J. Automob. Eng. 217 (7) (2003) 583–593.

[3] J. Axsen, A. Burke, K. Kurani, Batteries for Plugin Hybrid Electric Vehicles (PHEVs): Goals and State of the Technology, UC Davis, internal report, Davis, CA, 2008.

[4] N. Omar, B. Verbrugge, P. Van den Bossche, J. Van Mierlo, Power and life enhancement of battery-electrical double layer capacitor for hybrid electric and charge-depleting plug-in vehicle applications, Electrochim. Acta 55 (2010) 7524–7531.

[5] P. Van den Bossche, F. Vergels, J. Van Mierlo, J. Matheys, W. Van Autenboer, SUBAT: an assessment of sustainable battery technology, J. Power Sources 162 (2) (2006) 913–919.

[6] J. Axsen, K.S. Kurani, A. Burke, Are batteries ready for plug-in hybrid buyers? J. Transp. Policy 17 (2010) 173–180.

[7] N. Omar, M. Daowd, B. Verbrugge, G. Mulder, P. Van den Bossche, J. Van Mierlo, M. Dhaens, S. Pauwels, F. Leemans, Assessment of performance characteristics of lithium-ion batteries for PHEV vehicles applications based on a newly test methodology, in: The 25th World Battery, Hybrid and Fuel Cell Electric Vehicle Symposium, November 5–9, 2010, Shenzhen, China, 2010.

[8] N. Omar, B. Verbrugge, G. Mulder, P. Van den Bossche, J. Van Mierlo, M. Daowd, M. Dhaens, S. Pauwels, Evaluation of performance characteristics of various lithium-ion batteries for use, in: VPPC 2010, Lille, ISBN 978-1-4244-8220-7, 2010.

[9] N. Omar, M. Daowd, G. Mulder, J.M. Timmermans, P. Van den Bossche, J. Van Mierlo, S. Pauwels, Assessment of performance of lithium iron phosphate oxide, nickel manganese cobalt oxide and nickel cobalt aluminum oxide based cells for using in plug-in battery electric vehicle applications, in: VPPC 2011, September 6–9, 2011, Chicago, 2011.
[10] G.H. Kim, J. Gonder, J. Lustbader, A. Pesaran, Thermal management of batteries in advanced vehicles using phase-change materials, World Electr. Veh. J. 2 (2008) 46–59.
[11] D.H. Doughty, P.C. Butler, R.G. Jungts, E.P. Roth, Lithium battery thermal models, J. Power Sources 110 (2002) 357–363.
[12] N. Omar, M. Abdel Monem, Y. Firouz, J. Salminen, J. Smekens, O. Hegazy, H. Gualous, G. Mulder, P. Van den Bossche, Th. Coosemans, J. Van Mierlo, Lithium iron phosphate based battery—assessment of the aging parameters and development of cycle life model, J. Appl. Energy 113 (2014) 1575–1585.
[13] N. Omar, Assessment of rechargeable energy storage systems in plug-in hybrid electric vehicles, Ph.D. dissertation, Vrije Universiteit Brussel, Brussels, Belgium, 2012.
[14] J. Wang, P. Liu, J. Hicks-Garner, E. Sherman, S. Soukiazian, M. Verbrugge, H. Tataria, J. Musser, P. Finamore, Cycle-life model for graphite-$LiFePO_4$ cells, J. Power Sources 196 (2011) 3942–3948.
[15] E. Eddahech, O. Briat, E. Woirgard, J.M. Vinassa, Remaining useful life prediction of lithium batteries in calendar ageing for automotive applications, Microelectron. Reliab. 52 (2012) 2438–2442.
[16] R.B. Wright, C.G. Motloch, J.R. Belt, J.P. Christophersen, C.D. Ho, R.A. Richardson, I. Bloom, S.A. Jones, V.S. Battaglia, G.L. Henriksen, T. Unkelhaeuser, D. Ingersoll, H. L. Case, S.A. Rogers, R.A. Sutula, Calendar- and cycle-life studies of advanced technology development program generation 1 lithium-ion batteries, J. Power Sources 110 (2002) 445–470.
[17] A. Eddahech, O. Briat, R. Chaari, N. Bertrand, H. Henry, J.M. Vinassa, Lithium-ion cell modeling from impedance spectroscopy for EV applications, in: IEEE Energy Conversion Congress and Exposition Conference, Phoenix, AZ, 2011.
[18] Q. Zhang, R.E. White, Calendar life study of Li-ion pouch cells. Part 2: simulations, J. Power Sources 179 (2008) 785–792.
[19] K. Kassem, J. Bernard, R. Revel, S. Pélissier, F. Duclaud, C. Delacourt, Calendar aging of a graphite/$LiFePO_4$ cell, J. Power Sources 208 (2012) 296–305.
[20] G. Mulder, N. Omar, S. Pauwels, F. Leemans, B. Verbrugge, W. De Nijs, P. Van den Bossche, D. Six, J. Van Mierlo, Enhanced test methods to characterise automotive battery cells, J. Power Sources 196 (2011) 10079–10087.
[21] N. Omar, M. Daowd, O. Hegazy, G. Mulder, J.M. Timmermans, Th. Coosemans, P. Van den Bossche, J. Van Mierlo, Standardization work for BEV and HEV applications: critical appraisal of recent traction battery documents, Energies 5 (2012) 138–156.
[22] M. Broussely, S. Herreyre, P. Biensan, P. Kasztejna, K. Nechev, R. Staniewicz, Aging mechanism in Li ion cells and calendar life predictions, J. Power Sources 97–98 (2001) (2011) 13–21.
[23] H.J. Phoehn, P. Ramadass, R.E. White, Solvent diffusion model for aging of lithium-ion battery cells, J. Electrochem. Soc. 151 (2004) A456–A462.
[24] W. Bögel, J.P. Büchel, H. Katz, Real-life EV battery cycling in the test bench, J. Power Sources 72 (1998) 37–42.
[25] P. Liu, J. Wang, J. Hicks-Garner, E. Sherman, S. Soukiazian, M. Verbrugge, H. Tataria, J. Musser, P. Finamore, Aging mechanisms of $LiFePO_4$ batteries deduced by electrochemical and structural analyses, J. Electrochem. Soc. 157 (2010) A499e–A507e.

[26] J. Schmalstieg, S. Käbitz, M. Ecker, D. Uwe Sauer, A holistic aging model for Li(NiMnCo)O_2 based 18650 lithium-ion batteries, J. Power Sources 257 (2014) 325–334.
[27] N. Omar, H. Gualous, M. Al Sakka, J. Van Mierlo, P. Van den Bossche, Electric and thermal characterization of advanced hybrid Li-ion capacitor rechargeable energy storage system, in: Proceedings 4th International Conference on Power Engineering, Energy and Electrical Drives, Istanbul, Turkey, 2013.
[28] F. Rafik, H. Gualous, R. Gallay, A. Crausaz, A. Berthon, Frequency, thermal and voltage supercapacitor characterization and modeling, J. Power Sources 165 (2007) 928–934.
[29] Q. Zhang, R.E. White, Calendar life study of Li-ion pouch cells, J. Power Sources 173 (2007) 990–997.
[30] R.G. Jungst, G. Nagasubramanian, H.L. Case, B.Y. Liaw, A. Urbina, T.L. Paez, D.H. Doughty, Accelerated calendar and pulse life analysis of lithium-ion cells, J. Power Sources 119–121 (2003) 870–873.
[31] N. Dupré, J.F. Martin, J. Degryse, C. Fernandez, P. Soudan, D. Guyomard, Aging of the $LiFePO_4$ positive electrode interface in electrolyte, J. Power Sources 195 (2010) 7415–7425.
[32] M. Wohlfahrt-Mehrens, C. Vogler, J. Garche, Aging mechanisms of lithium cathode materials, J. Power Sources 127 (2004) 58–64.
[33] S. Käbitz, J. Bernhard Gerschler, M. Ecker, Y. Yurdagel, B. Emmermacher, D. André, T. Mitsch, D. Uwe Sauer, Cycle and calendar life study of a graphite|$LiNi_{1/3}Mn_{1/3}Co_{1/3}O_2$ Li-ion high energy system. Part A: full cell characterization, J. Power Sources 239 (2013) 572–583.